

Trends in Extremes of Surface Humidity, Temperature, and Summertime Heat Stress in China

Julian X.L. Wang^{①②} and Dian J. Gaffen

NOAA/ Air Resources Laboratory, Silver Spring, MD, 20910, USA

(Received September 1, 2000)

ABSTRACT

In the past half century, the mean summertime temperature in China has increased, with nights warming more than days. Using surface station observations, we show that the frequency of extreme heat–stress events in China, caused by extremely hot and humid days as well as by heatwaves lasting for a few days, has increased over the period from 1951 to 1994. When humidity is high, hot weather can cause heat stress in humans. The increased heat–stress trend may pose a public health problem.

Key words: Trend detection, Climate change, Public health

1. Introduction

Previous studies have shown climatological and seasonal surface temperature and humidity distributions over China (Wang and Gaffen, 2001) and evaluated trends in seasonal means of several surface humidity variables, rainfall, temperatures, and apparent temperature for the last half century (Easterling et al., 2000, Zhai et al., 1999, Zhai and Eskridge, 1997, Zhai and Ren, 1997, Wang and Gaffen, 2001). However, trends in local temperatures, and particularly trends in extreme heat events have a more direct effect on human populations. Extreme hot weather is associated with productivity losses and increased energy demanding. Heat waves are often accompanied by episodes of poor air quality, with greater human health impacts. Human mortality increases have been associated with temperatures in excess of local threshold values in cities around the world (WHO, 1996).

Few studies have reported long–term changes in the frequency of extreme heat events. In the U.S., small increases in mean summertime temperature during the past half century, accompanied by increases in surface humidity (Gaffen and Ross, 1999), have been associated with significant increases in extreme single–day heat stress events and multi–day heat waves (Gaffen and Ross, 1998). We will present a comparable analysis of temperature, humidity, and summertime extreme heat for China, where heat waves can be a more serious concern due to its large population with insufficient supply of energy.

Due to increases in greenhouse gases, an increase in tropospheric water vapor concentrations is an expected climate change signal (Kattenberg et al., 1995). Zhai and Eskridge (1997) showed increases in tropospheric precipitable water in China based on radiosonde data. In our previous report (Wang and Gaffen, 2001), we have presented evidences of increase trends in surface temperature, specific humidity, and apparent temperature, a measure of human

^①Corresponding author address: Julian X.L. Wang, NOAA Air Resources Laboratory, R/ ARL, 1315 East West Highway, Silver Spring, MD 20910, USA.

^②E–Mail: julian.wang@noaa.gov

comfort combining both temperature and humidity developed by Steadman (1984), by analyzing six-hourly surface meteorological observations from 196 stations in China (Kaiser, 1991). A relatively detailed description of the observing system and data quality control process were also given in Wang and Gaffen (2001).

2. Data

Surface meteorological data analyzed here were extracted from a database of weather observations from China Meteorological Administration (Wang and Gaffen, 2001). Six-hourly observations [0200, 0800, 1400, and 2000 Beijing Time (BT)], i.e., 1800, 0000, 0600, and 1200 UTC, of surface temperature and humidity are available from 196 Chinese stations covering the period 1951–1994.

We use only the 0600 UTC (1400 BT), observations to represent daytime value. The 0000 UTC (0800 BT) observation is excluded from daytime value, since, for a portion of the year at stations significantly west of Beijing, it is certainly not day-light at 0000 UTC (0800 BT). Likewise, the only 1200 UTC (0200 BT) observations are used for night time value at all stations.

A commonly used measure of human heat stress combines efforts of temperature and humidity. For consistence in analysis, we present temperature and humidity trends in the same way as for extreme heat and heat waves in the next section.

A relatively stable network of stations, and consistency in operational procedures since 1961, ensure that the quality of surface observations in China, for climate studies, is generally good. Some quality controls are performed to eliminate obvious errors due to station re-location and gross errors in data handling processes (Wang and Gaffen, 2001). In all cases, the quality control process was to reduce the magnitude of trends in the data. Trends are analyzed using nonparametric method of median of pairwise slopes regression (Lanzante, 1996), which is resistant to outliers in the time series and robust to non-normal data distributions (Wilks, 1995). This method of trend estimation is also less sensitive to length of the data series, and therefore, trend estimates of temperature and humidity extremes presented in this paper are relatively robust.

3. Trends in extremes of temperature and humidity

In the last half of the 20th century, the mean temperature in China has increased (Wang and Gaffen, 2001), with more warming during nighttime than daytime and more warming in winter than in summer. Moisture or specific humidity increases are most evident in summer. Increases in mean temperature and humidity are often accompanied by an increased frequency of days with extremely high temperature and humidity.

As discussed in Kalkstein and Davis (1989) and Gaffen and Ross (1998), the 85th percentile values of temperature and humidity derived from summer time (July–August) climatological data were used to compute frequencies of extremely high temperature and humidity for all months. Similarly, the 15th percentile values of temperature and humidity derived from winter time (January–February) climatological data are used to compute frequencies of extremely low temperature and humidity for all months. Based on those time series of extremes, trends are estimated using the nonparametric method of the median of pairwise slopes regression (Lanzante, 1996).

Presented in Fig. 1 are the 85th percentile values for temperature (Fig. 1a) and specific

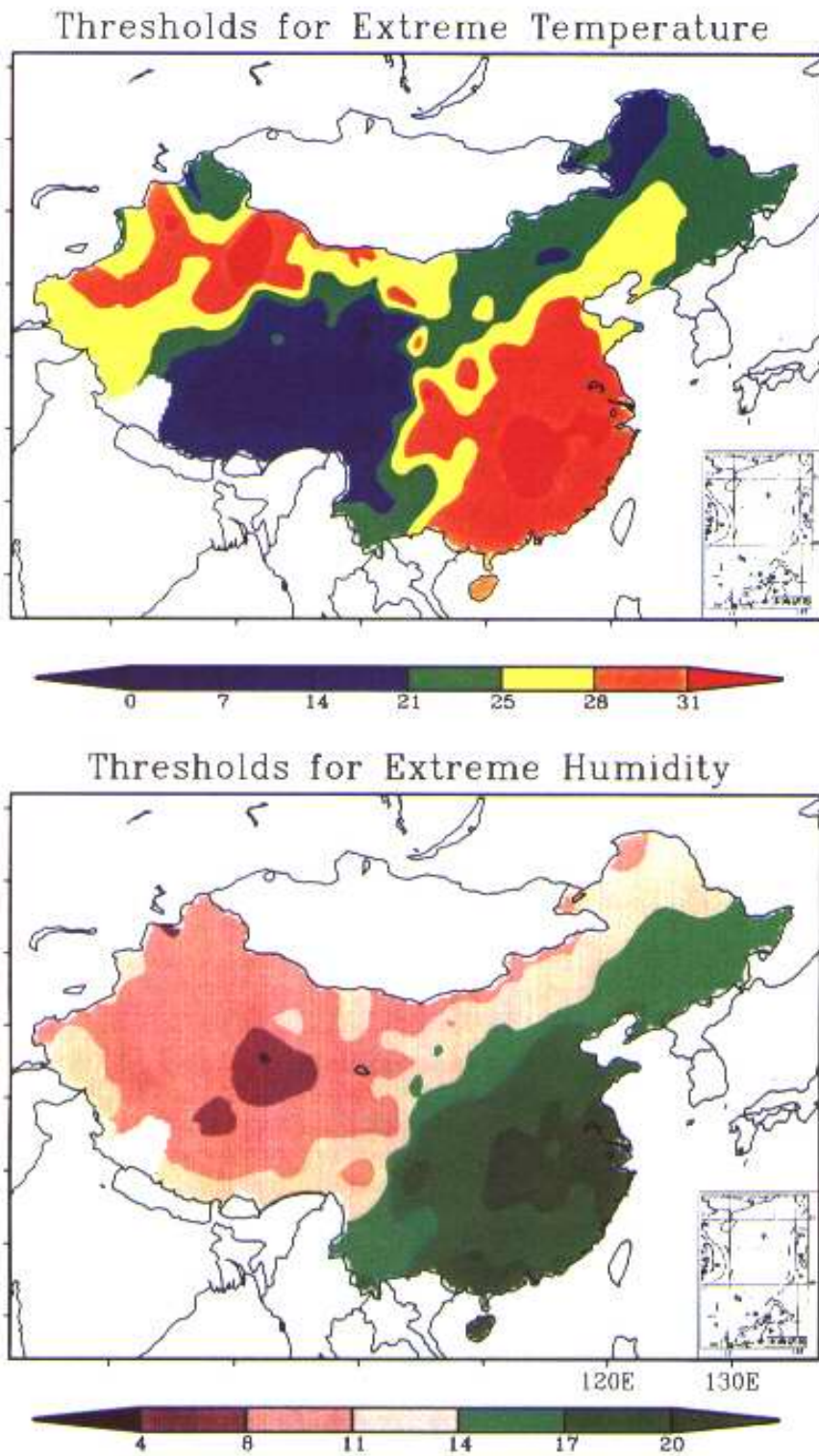


Fig. 1. Spatial pattern of threshold values of nighttime surface temperature (a) and surface humidity (b) during the summer (July–August) used for identification of extreme events in the China. Units are $^{\circ}\text{C}$ for the temperature and g/kg for the specific humidity.

humidity (Fig. 1b) using full-day observations, respectively. The local temperature thresholds (Fig. 1a) range from more than 31°C in Eastern–Southeastern China to less than 7°C over the Tibetan Plateau. The temperature thresholds are also high over the desert region of northwest China. For specific humidity, high thresholds are in the eastern half of country close to coasts and low humidity thresholds are in the western interior of the country. More than 20 g · kg⁻¹ high specific humidity values of the 85th percentile local thresholds are located around the southern coast and Yangtze River delta. For both temperature and humidity, the local thresholds are high in Sichuan basin adjacent to the Tibet Plateau with highest temperature and humidity gradient in between. Separate calculations of the thresholds for daytime and nighttime (figures not shown) show only small differences from the daily mean thresholds shown in Fig. 1, for both magnitudes and pattern distributions.

The nighttime trends of the frequency in exceeding these temperature and specific humidity thresholds are presented in Fig. 2. Of the 196 stations, there are 140 stations (71%) with positive trends for temperature (Fig. 2a) and 153 stations (78%) with positive trends for specific humidity (Fig. 2b). A majority of stations with significant trends in both temperature and specific humidity have positive trends. The largest increase trends for both temperature and specific humidity are located around the southeastern coast, the northern border close to Mongolia, and much of highland in western China. The trends are generally weak in the Yellow River and Yangtze River basins and in the coastal eastern China.

One silent feature when comparing Figs. 2a and 2b is that a very few stations have negative trends in both temperature and specific humidity. Over southeastern China, where is densely populated and high extremes are controlled by summer monsoon system, the increase trends in both specific humidity and temperature are equally important. For northwestern China, more stations have positive humidity trends than temperature trends.

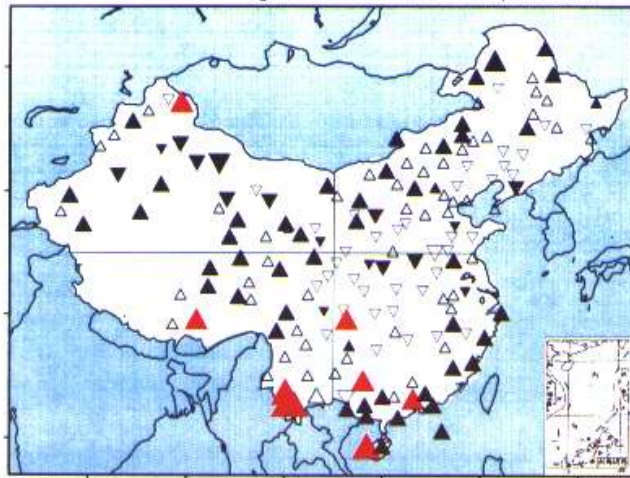
One interesting point to note is that while both temperature and humidity threshold values are highest in middle–lower Yangtze River basin (east of 105°E), the trends are obviously a mixture of weak positive and negative with larger increase trends to its north and south.

The nighttime trends shown in Fig. 2 are largest in comparison to trends of daytime observations and all-day averages. Statistically significant regions for daytime trends and all-day averaged trends are also much smaller (figures not shown).

Time series of national mean extreme temperature and specific humidity are shown in Figs. 3a and 3b (top panel), along with trends. On average, there are about 13 days every year for temperature exceeding 85th percentile of July–August values, and 11 days for specific humidity. Temperature extreme has an increase trend of 1.2 days per decade which is about 10 percent of mean, while increase trend of specific humidity is about 0.8 days per decade. Also shown in Fig. 3 are time series of four regional averages, i.e., northeast, southeast, southwest, and northwest, defined by latitude line of 35°N and longitude line 105°E as shown in Fig. 2. The strongest temperature trends are in the southwest quadrant, where increase trend of extreme temperature reaches 2.2 days per decade. The strongest humidity trends are, however, in the northwest quadrant, a increase trend of 2.3 days per decade.

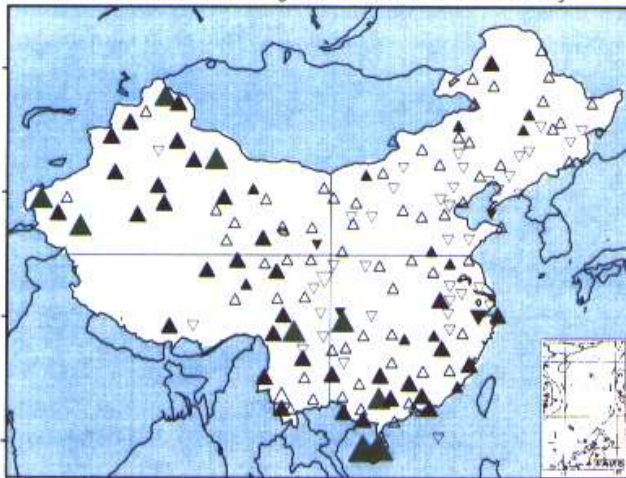
A similar analysis on lower extremes of temperature and specific humidity were also performed. Using 15th percentile values of January–February as the thresholds, colder (drier) extremes are defined as temperature (specific humidity) colder (lower) than the thresholds. Results (figures not shown) are consistent with the conclusions of warming trend in temperature and moistening trend in specific humidity as seen in Figs. 2 and 3.

Trend in Extreme Nighttime Surface Temperature



\blacktriangle < 2 days \blacktriangle 2-4 days \blacktriangle 4-6 days \blacktriangle > 6 days

Trend in Extreme Nighttime Surface Humidity



\blacktriangle < 2 days \blacktriangle 2-4 days \blacktriangle 4-6 days \blacktriangle > 6 days

Fig. 2. Decadal trends in the annual frequency of extreme nighttime surface temperature (a) and surface humidity (b) exceeding the thresholds shown in Fig. 1. Upward triangles are for positive trends and downward ones are for negative trend. Filled triangles indicates significant trends at 95% confidence level. Units are days per decade for both extremes of temperature and humidity.

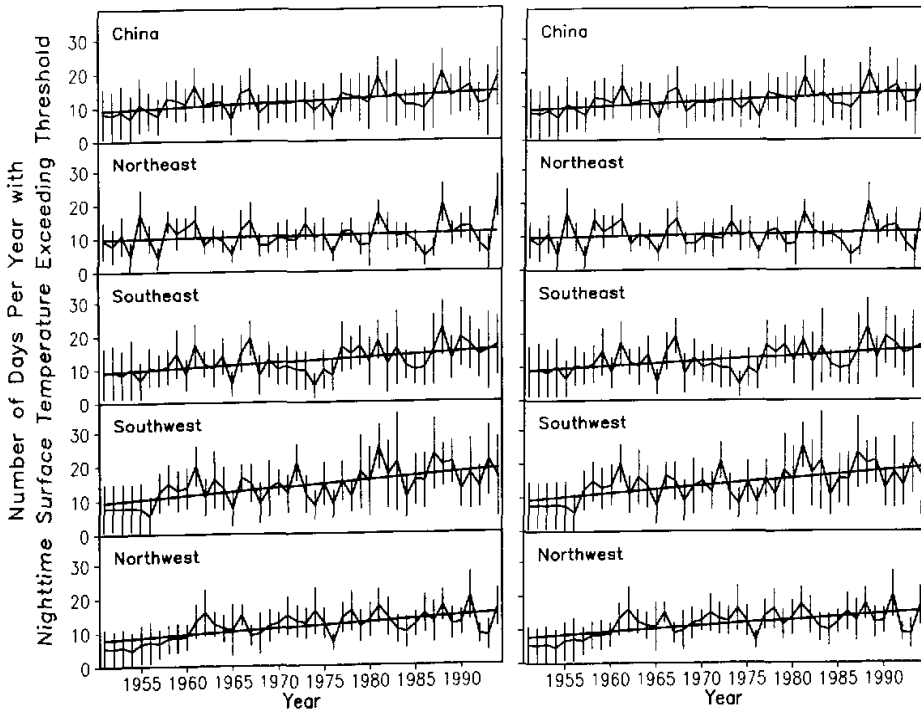


Fig. 3. Regional averaged time series of the annual frequency in extreme temperature (a) and humidity (b). Five panels are for whole China, Northeast, Southeast, Southwest, and Northwest, as indicated by the lines in Fig. 2. The vertical lines represents standard deviation of the region. The linear trend line is also shown.

4. Trends in extreme heat and heat wave

The combined efforts of temperature and humidity in sultry weather are incorporated in the 'apparent temperature' T_a , which is a widely used measure of human heat stress. In terms of ambient temperature and water-vapor pressure, T_a can be expressed as $T_a = -1.3 + 0.92T + 2.2e$, where T is surface temperature in $^{\circ}\text{C}$ and e is surface vapor pressure in millibar. (Steadman, 1984).

Following the same analysis of temperature and humidity, the climatology-based threshold for T_a are shown in Fig. 4. These thresholds are again based on data for July and August which are the hottest months, but they can be exceeded during any month of the year. Typically, they are exceeded about 12 times a year. Trends in the annual frequency of the nighttime apparent temperature exceeding local threshold values are shown in the bottom panel of Fig. 5. Trends for daytime and all-day average values are weaker and their statistical significant area are smaller (figures not shown).

Thresholds for Extreme Heat Stress

85th Percentile Value of July–August
Daily–average Apparent Temperature

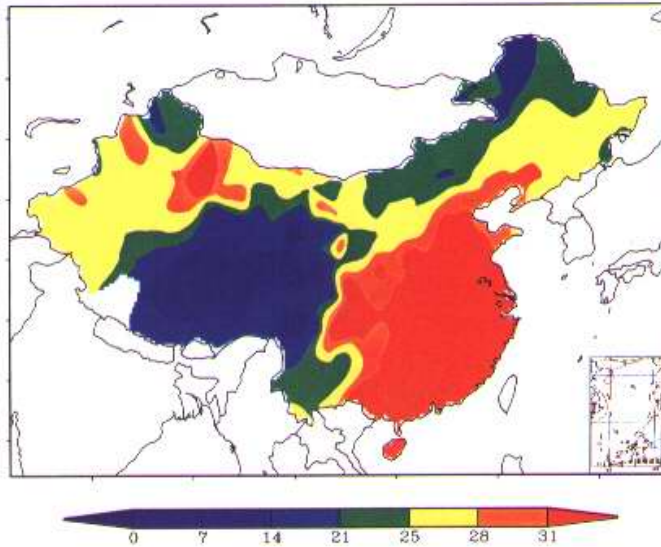


Fig. 4. Same as in Fig. 1, except for the extreme heat stress, as defined in the text.

1951–1994 Decadal Trends in the Annual Frequency of Extreme Nighttime Apparent Temperature

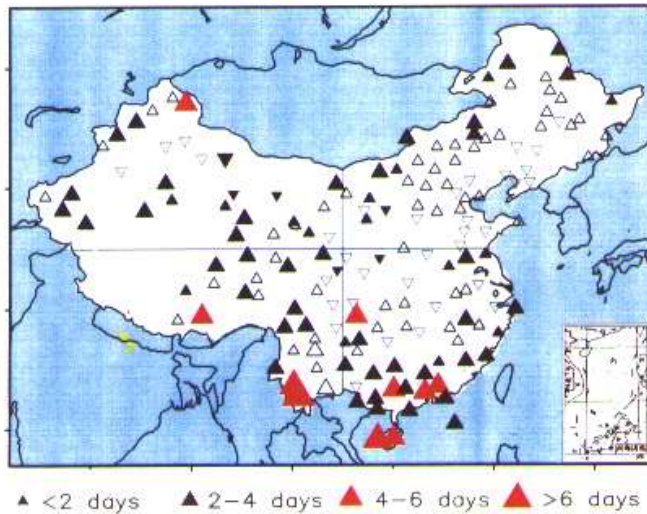


Fig. 5. Same as in Fig. 2, except for the extreme heat stress.

The threshold values for T_a are higher than that of temperature due to humidity effects. By comparison of Fig. 4 with Fig. 1a, it is clear that the largest humidity impacts on extreme apparent temperature, often called heat stress, are in the quadrants of southeast and to some extent northwest China. The highest heat stress thresholds over the southeastern China reach 34°C, which is a 3°C increase from 31°C of the highest surface temperature thresholds.

Trends in heat stress are very similar to those of temperature with relatively weak values in Yellow River and Yangtze River basins and coastal northeast China. Due to moisture contribution, there are 80 (156 out 196 stations) percent of stations showing increase trend in apparent temperature, which represents a nine percent increase from surface temperature alone. Most of increases are in southeast and northwest quadrants (Fig. 5).

On national average, trend in extreme heat stress is increasing at rate of 1.2 days per decade (Fig. 6a). The strongest trends are in southwest quadrant (2.2 days per decade). By comparison of trends in surface temperature and apparent temperature, the moisture contribution to heat stress results in a 15 percent increase of positive trend in southeast and northwest quadrants. In southeast, a trend of 1.3 days per decade in surface temperature is increased to 1.5 days per decade in apparent temperature, while in northwest values are changed from 1.5 days per decade to 1.7 day per decade.

Increase in single-day heat stress events are associated with increase in heat-waves, defined as runs of three or more consecutive days with daily averaged T_a exceeding the 85th percentile value. On average, each weather station experiences 2 three-day heat waves per year. Shown in Fig. 6b is the national and four regional averages of the heat waves. Also shown in Fig. 4 is the trend line of the heat waves. Upwards trends in the frequency of heat waves are significant at 95% confidence level in nationwide average and indicate an increase of about 73% in the number of 3-day heat waves over the period from 1951 to 1994. In southeast region where has the highest density of populations, increase of heat waves over entire period reaches 132%. The increases in number of heat waves are 114% for southwest region, i.e., Tibetan Plateau, 82% for northwest region, and lowest 23% in northeast region.

5. Discussion and conclusion

Upward trends are observed in both extreme temperature and extreme humidity, with larger trends at night than during the day. The trends in the extremes are consistent with results from previous studies of seasonal means (Wang and Gaffen, 2001) and maximum and minimum temperature (Karl et al., 1993, Easterling et al., 1997). Increases in summertime temperature and humidity lead to increases in apparent temperature. Defining extremes as events during which local thresholds of apparent temperature are exceeded, we find increases in the frequency of single-day extreme apparent temperature or heat stress during both nighttime and daytime. The occurrence of three-day heat waves increases significantly nationwide.

These trends may be partially associated with increased urbanization, especially over southeast region where has fast population growth and industrialization in last several decades. Extended urban heat island and air pollutant increase due to the urbanization and industrialization contribute to occurrences of more frequent extreme high temperature and heat waves, especially at night (Gallo et al., 1999). However, regional consistency of the trends suggests that their origins are not strictly local. This result is very comparable to the one over the US reported by Gaffen and Ross (1998).

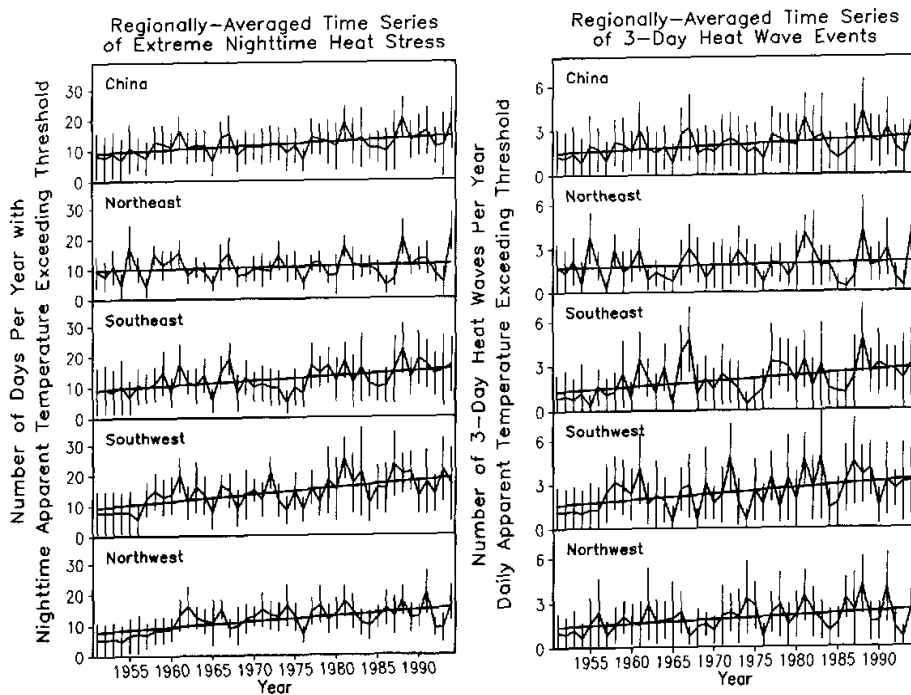


Fig. 6. Same as in Fig. 3, except for (a) heat stress and (b) 3-day heat waves.

If these climate trends continue they may pose a serious public health problem (McMichael, 1996). For example due to temperature increase, certain vector-transmitted infectious diseases which are usually restricted in southern China have emerged in many places of northern part of China with strong severity. Particularly as there are fast increasing numbers of elderly people in China, they are most vulnerable to heat-related sickness and mortality (Kalkstein and Davis, 1989).

REFERENCES

- Easterling, D.R., B. Horton, P.D. Jones, T.C. Peterson, T.R. Karl, D.E. Parker, M.J. Salinger, V. Razuyev, N. Plummer, P. Jamason, and C.K. Folland, 1997: Maximum and minimum temperature for the globe. *Science*, **277**, 264–366.
- Easterling, D.R., J.L. Evans, P. Ya. Groisman, T.R. Karl, K.E. Kunkel, and P. Ambenje, 2000: Observed variability and trends in extreme climate events: A brief review. *Bulletin of the American Meteorological Society*, **81**, 417–426.
- Gaffen, D.J., and R.J. Ross, 1998: Increased summertime heat stress in the US. *Nature*, **396**, 529–530.
- Gaffen, D.J., and R.J. Ross, 1999: Climatology and trends in US surface humidity and temperature. *J. Climate*, **12**,

- 811–828.
- Kaiser, D.P., 1991: Two long-term instrumental climatic data bases of the People's Republic of China. ORNL/CDIAC-47, Oak Ridge National Laboratory, Oak Ridge, TN.
- Kalkstein, L.S., and R.E. Davis, 1989: Weather and human mortality: An evaluation of demographic and interregional responses in the United States. *Ann. Assoc. Amer. Geogr.* **79**, 44–64.
- Kattenberg, A., and Coauthors, 1995: Climate models—Projections of future climate. *Climate Change 1995: The Science of Climate Change*, J.T. Houghton, L.G. Meira Filho, B.A. Callendar, N.Harris, A. Kattenberg, and K. maskell, Eds., Cambridge University Press, 285–357.
- Lanzante, J.R., 1996: Resistant, robust and nonparametric techniques for analysis of climate data: Theory and examples, including applications to historical radiosonde station data. *Intl. J. Climatol.*, **16**, 1197–1226.
- McMichael, A.J. 1995: *Climate Change 1995: Impacts, Adaptations and Mitigation of Climate Change*. Cambridge Univ. Press, 1996, 878pp.
- Steadamn, R.G., 1984: A universal scale of apparent temperature. *J. Clim. Appl. Meteor.*, **23**, 1674–1687.
- Wang, X. L., and D. J. Gaffen, 2001: Late twentieth century climatology and trends of surface humidity and temperature in China. *J. Climate*, **14**, 2833–2845.
- WHO, 1996: *Climate Change and Human Health*. A.J. McMichael, A. Haines, R. Sloof, and S. Kovats, eds., Geneva, 297pp.
- Zhai, P. M., and F. M. Ren, 1997: Change of maximum and minimum temperature during the past 40 years in China. *Acta Meteorologica Sinica*, **54**(4), 418–429.
- Zhai, P., and R. E. Eskridge, 1997: CAthmospheric water vapor over China. *J. Climate*, **10**, 2643–2652.
- Zhai, P., A. Sun, F. Ren, X. Liu, B. Gao, and Q. Zhang, 1999: Changes of climate extremes in China. *Climatic Changes*, **42**, 203–218.